Liquid Crystals
Publication details, including instructions for authors and subscription information:
http://www.informaworld.com/smpp/title~content=t713926090

Director patterns and inversion walls in 2D inhomogeneously deformed nematic LC layers

H. Schmiedel[a]; Ch. Cramer[a]; R. Stannarius[a]; K. Eidner[a]; M. Grigutsch[a]
[a] Fachbereich Physik der Universität Leipzig, Leipzig, Germany

To cite this Article Schmiedel, H. , Cramer, Ch. , Stannarius, R. , Eidner, K. and Grigutsch, M.(1993) 'Director patterns and inversion walls in 2D inhomogeneously deformed nematic LC layers', Liquid Crystals, 14: 6, 1935 — 1943
To link to this Article: DOI: 10.1080/02678299308027729
URL: http://dx.doi.org/10.1080/02678299308027729

LIQUID CRYSTALS, 1993, VOL. 14, NO. 6, 1935–1943

Director patterns and inversion walls in 2D inhomogeneously deformed nematic LC layers

by H. SCHMIEDEL, CH. CRAMER, R. STANNARIUS*, K. EIDNER
and M. GRIGUTSCH
Fachbereich Physik der Universität Leipzig,
Linnéstr. 5, O-7010 Leipzig, Germany

With progressing resolution of dot matrix displays, effects of inhomogeneous electric fields at the edges of structured electrodes become more and more important in the optical performance. We present a new method of polarizing microscopy for the study of the director field in two-dimensionally inhomogeneous nematic LC layers. Planar cells with electrode strips are investigated. The novel effects observed in these systems are two types of inversion walls, depending upon the preferred director orientation at the glass plates with respect to the electrodes.

1. Introduction

If electrode structures in LC display cells become comparable to the cell thickness, the inhomogeneity of the electric field near the electrode edges has to be considered in the static and dynamic characteristics of the display. Due to decreasing pixel sizes in modern display techniques (for example, screen projection displays) these effects are no longer negligible. In such geometry, several types of disclination lines appear which influence the optical properties of the device.

This paper is concerned with the analysis of the director field in thin nematic layers with planar boundary conditions and strip-shaped electrodes which give rise to a 2D inhomogeneous electrical field and director field in the LC material.

In the literature, several attempts have been made at theoretical descriptions of 2D and 3D inhomogeneously deformed director fields in nematics [1–5], but more effort seems to be necessary in their experimental investigation.

By means of polarizing microscopy, we have performed a study of the director field in structured, planar, non-twisted nematic cells. A novel method of polarizing microscopy is presented, where numerical signal processing allows the computer aided measurement of the director field. Special consideration is given to the distribution of the optical axes near the edges of the electrodes. It will be shown that the inhomogeneity of the director field in this region, under certain conditions, induces a twist deformation of the director field.

Furthermore, depending on the orientation of the electrode strips with respect to the undisturbed director, two different types of inversion walls occur above the Fréedericksz transition. A model is presented which describes the voltage dependence of the width and orientation of the resulting twist-bend walls in LC cells with electrode strips.

2. Sample geometry and LC material

The geometry of the LC cells is given in figure 1. These cells were manufactured and filled by JENOPTIC Jena. The length of the transparent electrode strips on the

---

* Author for correspondence.

0267–8292/93 $10·00 © 1993 Taylor & Francis Ltd.

upper glass plate is about 10 mm, which is large compared to their width g. Samples with $g = 100\,\mu$m and $g = 16\,\mu$m have been used. The electrode thickness has been determined by laser interferometry to be 30 nm. The projections of the director **n** on to the xy (see figure 1 (*a*)) and the xz plane (see figure 1 (*b*)) are shown.

Planar orientation of the director at the glass plates has been achieved by oblique evaporation techniques of SiO_x $(1 < x < 2)$ [6]. The pretilt given by the manufacturer is $0{\cdot}5 \pm 0{\cdot}5°$ and the twist angle at the surfaces is $0 \pm 3°$. If no voltage is applied, the director **n** is undisturbed and is determined by the planar boundary conditions. Two principal cases of alignment are considered, both of them without twist:

(i) director perpendicular to the strips ($\mathbf{n} = \mathbf{n}_s = (1, 0, 0)$; case n_s),
(ii) director parallel to the strips ($\mathbf{n} = \mathbf{n}_p = (0, 1, 0)$; case n_p).

After applying the voltage V to the electrodes, the director field is described by $\mathbf{n} = (\cos\theta\cos\varphi, \cos\theta\sin\varphi, \sin\theta)$ where the tilt angle θ and the twist angle φ both depend upon the spatial coordinates $\mathbf{r} = (x, y, z)$.

The material used was PCH5 (E.Merck) which is nematic in the temperature range from 30°C to 54·9°C and can be easily supercooled. Its viscoelastic, dielectric and optical parameters are well known [7, 8]. Using a birefringence of $\Delta n = 0{\cdot}1165$ for PCH5 at 30°C, the phase retardation Δ_L in the undisturbed LC cell of $7{\cdot}0\,\mu$m thickness is given $\Delta_L = 2\pi/\lambda \cdot \Delta n \cdot d = 8{\cdot}699$ at $\lambda = 589$ nm. If the cell is illuminated with white light and observed between crossed polarizers with the strips in the diagonal position, a greenish interference colour appears (cf. figure 2).

If we assume that the director field in the middle of the electrode strips is not affected by the inhomogeneous field at their edges, we can define a Fréedericksz threshold (which would correspond to the Fréedericksz transition of the bulk cell with non-structured electrodes). This threshold voltage was determined experimentally to be 0·93 V at 28°C in all cells investigated, in good agreement with theoretical data.

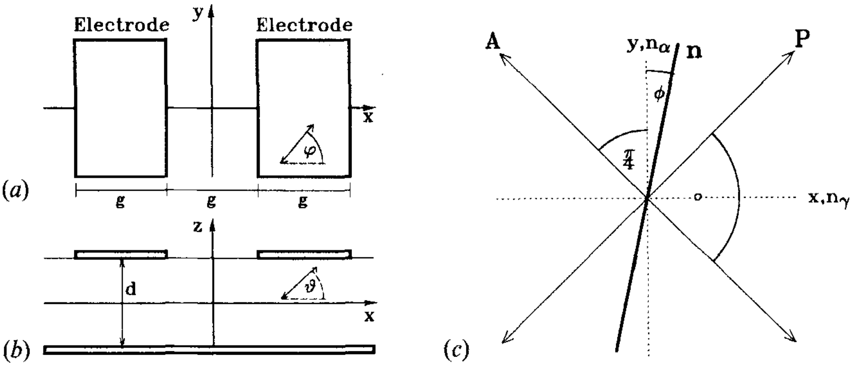

Figure 1. Cell geometry of the samples. The upper electrode consists of 20 parallel equidistant strips (two of them being shown in the figure) whereas the lower electrode is an unstructured plane. (*a*) top view, xy plane, (*b*) cross-section, xz plane. (*c*) Orientation of the director field between crossed polarizers. y is the direction of the electrode strips and $\Phi = \bar{\varphi}$ is the mean derivation of **n** from the original diagonal orientation. n_α and n_γ denote the main refractive indices of a quartz wedge which is placed above the LC cell, giving an additional phase retardation linearly increasing in the y direction (cf. figure 5).

3. Analysis of the director field

In this section we discuss the fundamental optics for the interpretation of the microscopic pictures, neglecting the inversion walls that arise in both geometries. This enables us to determine the director field in all regions far from the walls. The director field in the vicinity of the wall has to be discussed separately.

Whereas the undisturbed director field according to the surface alignment is not twisted, a twist is induced in case n_p with rising voltage near the edges of the electrodes (see figure 2). Thus, the director field is generally described by the twist and tilt angles $\varphi(x, z)$ and $\theta(x, z)$. The following discussion applies to both geometries n_p and n_s as well. The exact calculation of the optical properties will be given in a subsequent paper. A simple approximation, however, can be used for a good qualitative description. Neglecting wave guiding effects [9], mean twist and tilt angles $\bar{\varphi}$ and $\bar{\theta}$ can be evaluated by means of polarizing spectroscopy using the formula

$$I_A = I_P \sin^2\left(\frac{\Delta_L}{2}\right)\cos^2(2\Phi), \tag{1}$$

where $I_{A,P}$ are the light intensities just behind the crossed analyser and polarizer, respectively. Φ is the mean twist deviation of the director from the undistorted diagonal orientation and

$$\Delta_L = \frac{2\pi}{\lambda}(\bar{n}_e - n_o)\cdot d \tag{2}$$

is the mean phase retardation between the extraordinary (e) and ordinary (o) light waves, caused by the effective birefringence $\Delta n = \bar{n}_e - n_o$ where

$$\bar{n}_e = \frac{n_e n_o}{d}\int_{-d/2}^{d/2} \frac{dz}{\sqrt{(n_e^2 \sin^2\theta + n_o^2\cos^2\theta)}} \tag{3}$$

and n_e, n_o are the main refractive indices of the LC material (see figure 1 (*c*)).

The values of the mean azimuth Φ of $\mathbf{n}$ have been obtained from the positions of zero intensity $I_A = 0$ at different azimuthal orientations of the sample cell with respect to the polarizers, and the mean tilt angle $\bar{\theta}$ of the director has been determined from the local interference colours of the samples illuminated with white light (see figures 2 and 3). From figure 3 it can be seen that despite the parallel alignment (case $\mathbf{n}_p$) at the surfaces, the director field becomes twisted by 90° near the edges of the electrodes, whereas the mean tilt angle $\bar{\theta}$ changes continuously from 0 outside to its maximum value inside the electrode area.

Higher accuracy and resolution in the determination of the director field can be achieved using a monochromatic light source and a quartz wedge above the sample between the crossed polarizers (with its main axis n_γ in the x direction, see figure 1 (*c*) and 5). In figure 5 the top view of an n_s type cell is shown, illuminated with white light. Due to the quartz wedge, the interference colours change along the electrode axes y (which are parallel to the wedge axes). The phase retardation in the liquid crystal is no longer represented by the interference colour, but by the shift of the colour band in the y direction. Using monochromatic instead of white light, we observe intensity modulations instead of the colour palette.

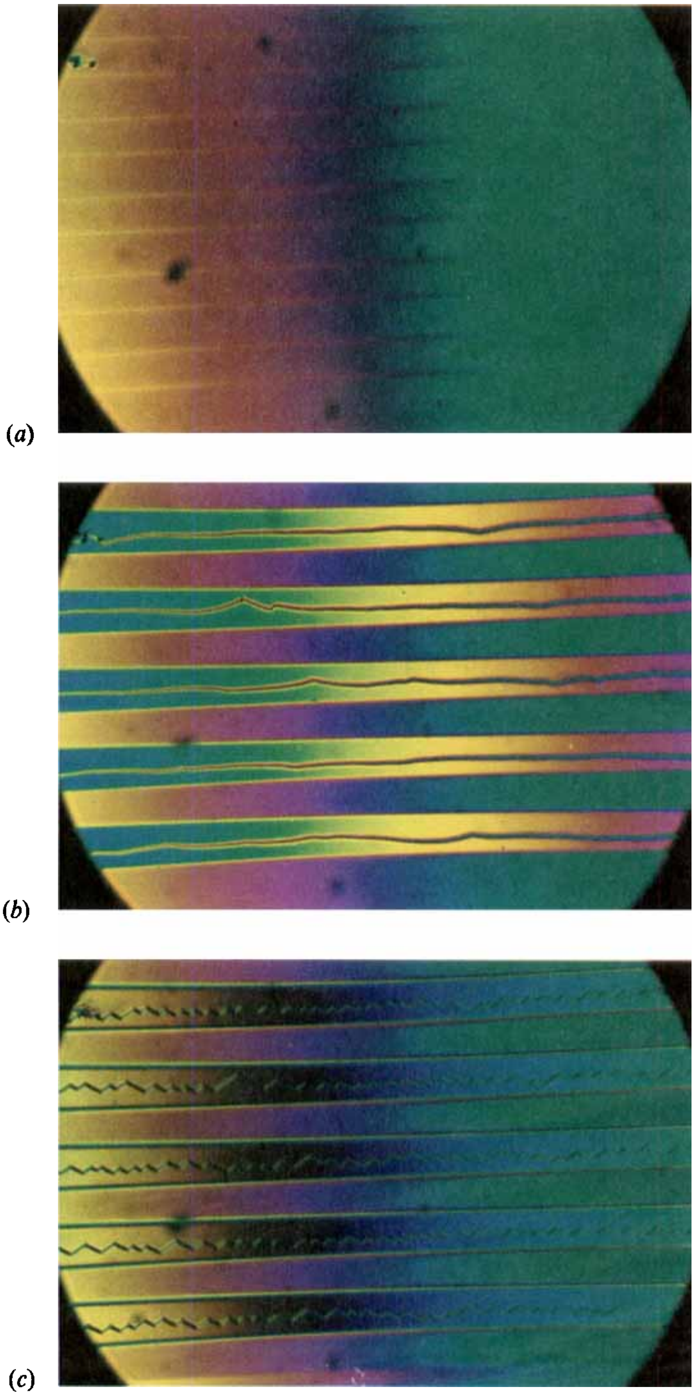

Figure 2. LC cell with electrode strips between crossed polarizers (case n_p, 7 μm cell thickness, PCH5, electrode widths 100 μm). Four (vertical) electrodes are shown on each picture. The greenish interference colour (in the inter-electrode areas) corresponds to the undisturbed director, $\theta=0$, $\varphi=90°$, whereas other colours correspond to a twisted and/or tilted director field. The small single lines in the electrode area are twist inversion walls, usually located near the middle of the electrodes but sometimes pinned to the edge (see second strip). These 'twist' walls arise after sudden application of a voltage to the cell. They separate regions with opposite senses of tilt. Voltages: (*a*) 1·28 V, (*b*) 1·77 V, (*c*) 5·26 V, temperature $T=25°$C.

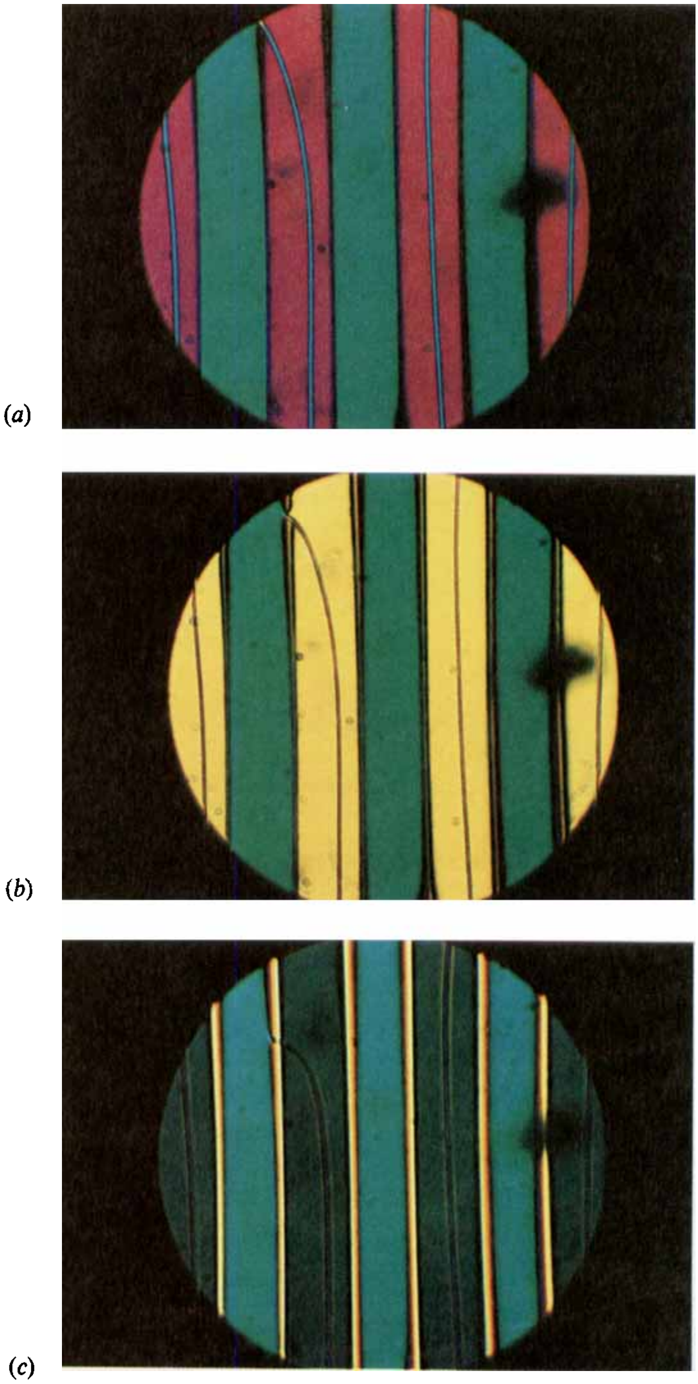

Figure 5. Top view of a cell with n_s geometry. (PCH5, $T=28°C$, $g=100\,\mu m$, quartz wedge above the sample, white light) (*a*) 0·95 V, (*b*) 1·45 V, (*c*) 2·12 V. Five (horizontal) electrodes can be seen. Due to the quartz wedge, the interference colour changes along the electrode axes. At the electrode areas, twist-bend inversion walls can be observed. The Fréedericksz threshold U_c is at 0·93 V. With increasing voltage, the twist-bend walls are deformed more and are more zig-zag-like. Their inclination angles are the same in all strips, being only a function of the applied voltage.

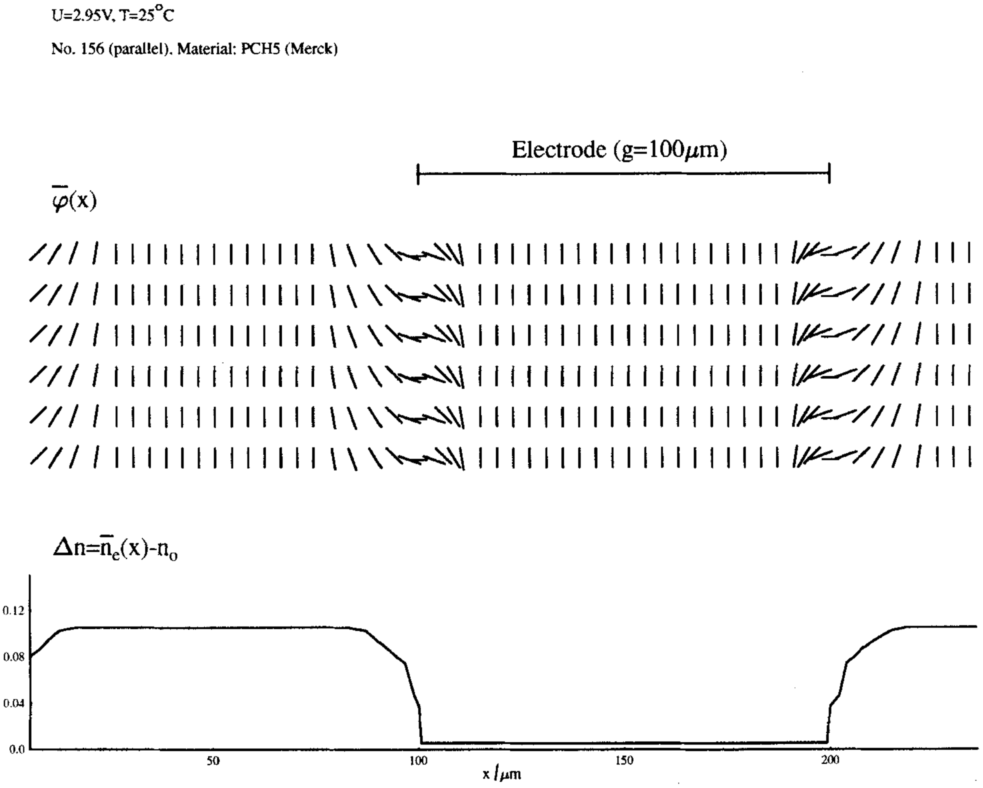

Figure 3. Behaviour of the mean twist Φ and mean birefringence Δn for case n_p ($T=25°C$, voltage 2·95 V, PCH5).

For monochromatic light the intensity I_A is given by

$$I_A=\frac{1}{2}I_P[1-a\cos(\Psi-\Delta_Q)], \tag{4}$$

where

$$a^2=1-\sin^2(4\Phi)\sin^4\left(\frac{\Delta_L}{2}\right) \tag{5}$$

and

$$\sin\Psi=\frac{\cos(2\Phi)\sin(\Delta_L)}{a}, \tag{6}$$

$\Delta_Q=2\pi/\lambda\cdot(n_{eQ}-n_{oQ})\cdot d_Q$ is the phase retardation introduced by the quartz wedge, increasing linearly in the y direction ($d_Q\propto|y|$).

According to equation 4, the intensity of the transmitted light is sinusoidally modulated in the y direction, where the modulation amplitude $a=a(x)$ and the phase shift $\Psi=\Psi(x)$ depend on the x direction perpendicular to the electrode strips (see figure 1). From both $a(x)$ and $\Psi(x)$, determined experimentally with a CCD camera, the mean azimuthal angle Φ and the mean tilt angle (or the corresponding phase retardation $\Delta_L(x)$) are evaluated using equations 5 and 6. As an example, the

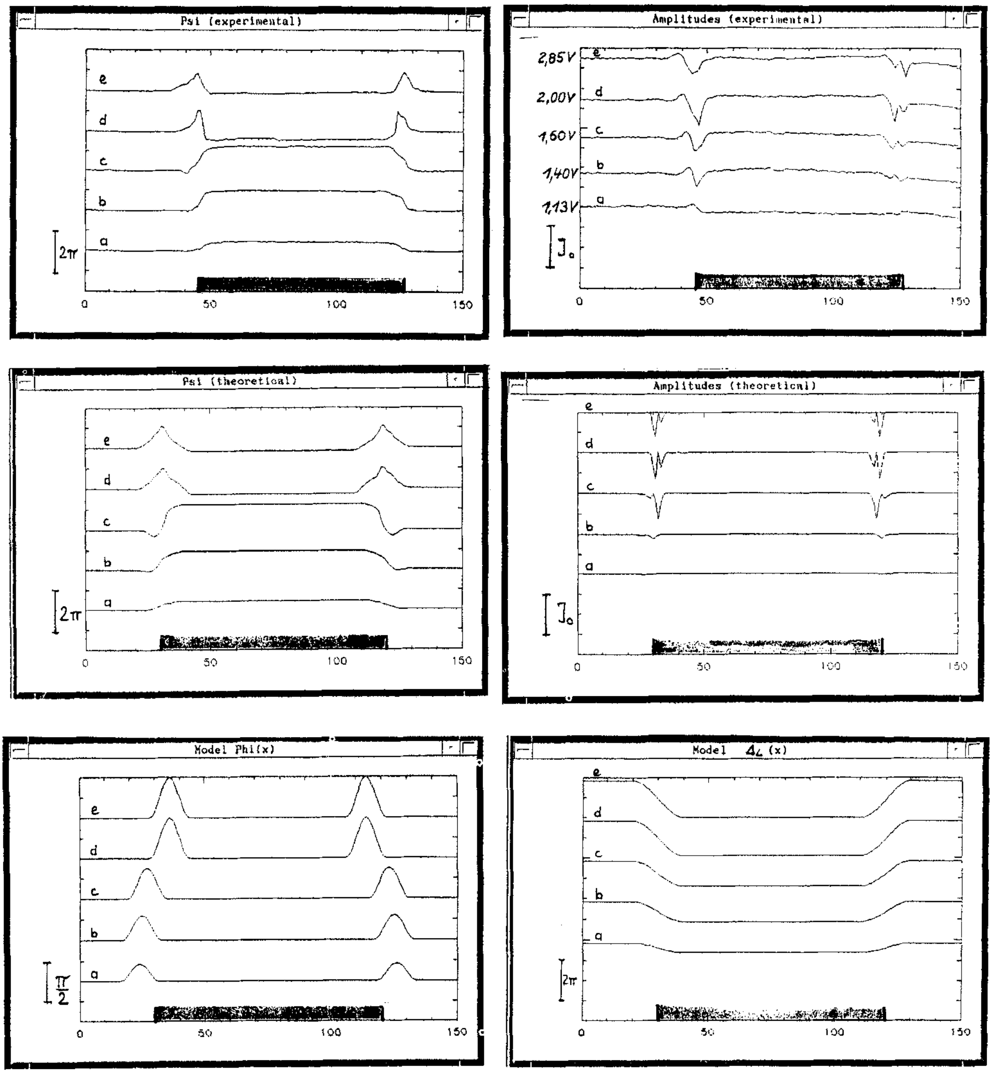

Figure 4. Experimental phase shift $\Psi(x)$ and modulation amplitude $a(x)$ of the intensity I_A (cf. equation (4)). The sample (case $\mathbf{n}_p$) together with a quartz wedge are placed between crossed polarizers. Curves a to e refer to different voltages. The range of the electrode cross-section is marked; numbers at the abscissa are arbitrary units.

experimental values of Ψ and a together with their theoretical values and the calculated twist angle and phase retardation, are presented in figure 4. The values of Φ and $\Delta_L(x)$ confirm the data obtained by conventional polarizing microscopy (see equation 1).

4. Inversion walls

Two different types of inversion walls can be observed. In case n_p, twist inversion walls arise in the region of the electrodes after a sudden application of sufficiently high voltages. These walls tend to be unstable and vanish at higher voltages or

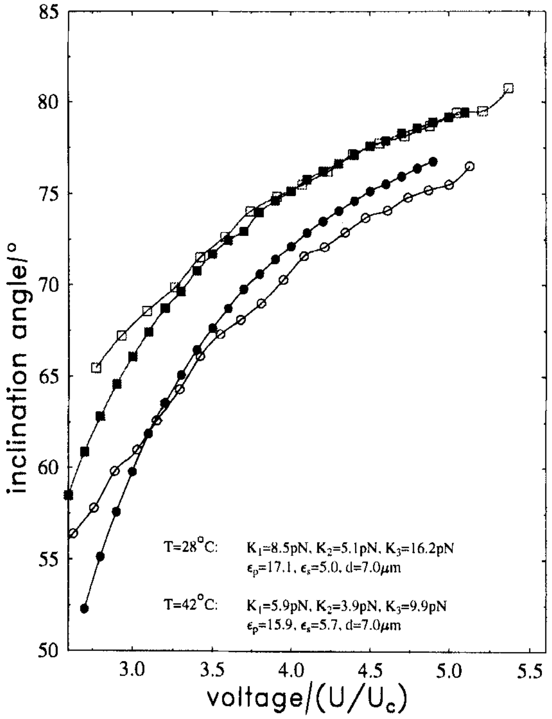

Figure 6. Experimental (empty markers) and theoretical (filled markers) values of the inclination angle α of the twist-bend inversion wall for $T=28°C$ and $T=42°C$ versus reduced voltage U/U_c. $U_c=\pi(K_1/(\varepsilon_0\varepsilon_a))^{1/2}$ is the Fréedericksz threshold, and K_1, K_2, K_3 and the cell thickness d are given in the figure. ○, Experimental at $T=28°C$; ●, theoretical at $T=28°C$; □, experimental at $T=42°C$; ■, theoretical at $T=42°C$.

temperatures (cf. see figure 2). In contrast in the geometry n_s, stable twist-bend walls are necessarily generated, forming zig-zag lines near the middle of the electrode (see figure 5). In this section we will discuss the latter geometry only. We will show a relationship between the zig-zag angle α formed by the linear parts of the walls with the electrode axis, and liquid crystal material constants. As this angle is reproducible, it allows in principle the determination of ratios of elastic constants as shown below.

The angle α does not depend upon the electrode width ($g=100\,\mu m$, $16\,\mu m$), but changes definitely with the applied voltage and temperature (see figure 6). Inversion walls in dielectrically deformed LC layers with planar boundary orientation were investigated earlier by Stieb *et al.* [10]. Whereas in extended LC layers these walls form closed lines, in the case of electrode strips, regions of opposite tilt are generated necessarily near the edges of the electrodes which force the walls to remain inside the electrode strips. By this mechanism, these walls are guided along the strip, tending to form an angle $\alpha < 90°$ to the x axis. The free energy of the walls is reduced in this case by partial replacement of splay and bend deformation energy by the energetically lower twist deformation [11].

Using these ideas, we were able to calculate the angle α and the wall thickness d_w independence upon the applied voltage and the cell temperature. The method will be described in detail in a subsequent paper. It is based on the computation of the free energy minimum per unit length of the electrode strip. The model ansatz for tilt and twist angles are

$$\theta(\xi, z)=\theta_0(z)\theta(\xi),$$

and

$$\varphi(\xi,z)=\varphi_1 \cos\left(\frac{\pi\xi}{d_w}\right)\cos\left(\frac{\pi z}{d}\right),$$

where ξ is the coordinate perpendicular to the local orientation of the twist-bend wall, $\pm\ \theta_0(z)$ is the solution for the undisturbed Fréedericksz transition, far from the wall, and θ satisfies the conditions $\theta(\pm d_w/2)=\pm 1$, providing a continuous change of the tilt angle from a negative to a positive sense of orientation across the twist wall. φ_1 resembles an induced non-zero twist in the inversion wall. The ansatz for the electrical potential in the wall $U(\xi, z)$ accounts for the distortion of the electric field due to the director deformation. The minimum of the functional for the free energy per unit length has been obtained by variation of the free parameters d_w, φ_1, θ and α. It can be seen from figure 6 that the experimental values of the inclination angle are described satisfactorily by this theory. Further details concerning the wall thickness d_w and the induced twist φ_1 will be published later.

5. Conclusions

A novel method of polarizing microscopy allowing computer-aided mapping of the director field in 2D inhomogeneously deformed liquid crystal layers has been presented and applied to planar cells with electrode strips. Near the edges of the electrodes, the inhomogeneity of the electrical field, together with the elastic energy, induces twist deformations of the director field irrespective of the planar and non-twisted surface alignment along the electrodes.

Whereas the twist inversion walls in samples with surface director orientation parallel to the electrode strips are rather unstable, twist-bend inversion walls in samples where the director is aligned perpendicular to the electrode strips are very stable. The latter necessarily arise above the Fréedericksz transition; they form zig-zag lines, the inclination angle of which depends on the elastic constants, the dielectric anisotropy, the thickness of the layer and the applied voltage. Using the variational principal of the free energy of the sample, the director field within the wall can be described satisfactorily with a simple model.

This work has been supported by the Deutsche Forschungsgemeinschaft under research number Schm 902/2-1.

References

[1] Chigrinov, V., 1990, *Molec Crystals liq. Crystals*, **179**, 71.

[2] Haas, G., Wöhler, H., Fritsch, M., and Mlynski, D. A., 1991, *Molec Crystals liq. Crystals*, **198**, 15.

[3] Haas, G., 1991, *Freiburger Arbeitstagung Flüssige Kristalle*, Proceedings P24.

[4] Dickmann, S., Cossalter, O., Eschler, J., and Mlynski, D. A., 1992, *Freiburger Arbeitstagung Flüssige Kristalle*, Proceedings P04.

[5] Schmidt, M., 1991, *Molec Crystals liq. Crystals*, **206**, 65.

[6] Cognard, J., 1982, *Molec Crystals liq. Crystals Suppl.*, **1**, 1.

[7] Finkenzeller, U., Geelhaar, T., Weber, G., and Pohl, L., 1989, *Liq. Crystals*, **5**, 313.

[8] Scharkowski, A., 1990, Dissertation Leipzig.

[9] Ong, H. L., and Meyer, R. B., 1985, *J. opt. Soc. Am.* A, **2**, 198.

[10] Stieb, A., Baur, G., and Meier, G., 1979, *Ber. Bunsenges. phys. Chem.*, **78**, 899.

[11] Brochard, F., 1992, *J. Phys., Paris*, **33**, 607.